



# A new approach based on a combination of capacitance and near-infrared spectroscopy for estimating the moisture content of timber

Vu Thi Hong Tham<sup>1,2</sup> · Tetsuya Inagaki<sup>1</sup> · Satoru Tsuchikawa<sup>1</sup>

Received: 21 March 2018 / Published online: 27 March 2019  
© Springer-Verlag GmbH Germany, part of Springer Nature 2019

## Abstract

The moisture content (MC) of wood influences its material properties. Determination of MC is essential in both the research and manufacturing fields. This study examined a nondestructive method for estimating MC rapidly and effectively. A capacitance sensor and a near-infrared (NIR) spectrometer were used to measure the MC of Japanese cedar and Japanese cypress timber. High-frequency capacitance (20 MHz) and NIR spectral absorption (908–1676 nm) data were collected for cross section and tangential section, as well as for the whole-sample average, in two MC ranges: from the green to the fiber saturation point (FSP) and from FSP to air-dried state. The results indicated that when standard error of prediction (SEP) is compared, the performance in [FSP to air-dried state] was better; when coefficient of determination in cross-validation ( $R^2_{\text{val}}$ ) and residual predictive deviation in cross-validation ( $\text{RPD}_{\text{val}}$ ) were compared, the performance in [Green to FSP] was better. Statistical analysis was performed using multiple linear regression and partial least squares. Combining capacitance and NIR absorbance at two wavelengths (Capacitance + NIR-MLR calibration) from the green to FSP was the best calibration yielding the most promising results:  $R^2_{\text{val}} = 0.96$ ,  $\text{SEP} = 5.20\%$  and  $\text{RPD}_{\text{val}} = 4.97$  on the cross section of samples. The results were higher than those of other calibrations in  $R^2$  and SEP and RPD values. The NIR-PLS calibration performed better than others with quite good  $R^2$ , lower SEP and higher RPD in the MC range from FSP to air-dried state. The first calibration using only capacitance of wood was good in the first range of MC, but it is not good in the second range ( $R^2$  under 0.5). Depending on the MC range, the performance of each calibration was different. In both MC ranges, the results on the cross section were higher than on the tangential section due to the anisotropic characteristics of wood material. From Capacitance + NIR-MLR calibration, the predicted models were developed using multiple linear regression and logarithmic regression. Results suggest the possibility of developing a new portable device combining a capacitance sensor and NIR spectroscopy to accurately predict the MC of wood.

## Introduction

Wood is a valuable, renewable resource possessing a variety of end-use applications. Rapid and reliable methods are needed to assess wood quality at all processing stages. In particular, it is important to correctly measure and predict moisture content (MC) of timber at the sawmill in order to control and treat the material effectively. Monitoring of the drying process from the green wood to the air-dried state helps us to understand the phenomena that cause cracking, shrinkage and deformation. The MC also influences fungal wood decay (Thybring 2013; Stienen et al. 2014; Meyer and Brischke 2015). Research by Thybring et al. (2018) provided insights into the chemical wood–water interactions and information on water distribution in the macro-void wood structure in wood material in the entire moisture range from dry to fully saturated state. Various protocols for assessment of MC are in use. There are two types of portable electric meter in widespread use today by researchers: resistance sensors and dielectric (capacitance) sensors (Wengert 1997). Capacitance sensors (one of the most common type of contact sensor for moisture measurement) are often used with biomaterials, because they are of low cost and easy to use and provide reasonably accurate measurements. Their functionality is based on the large difference in the dielectric constant between wood and water. Samples of seven western softwood species and white oak, conditioned to various levels of MC equilibrium, were inspected by Milota (1994) for MC using a capacitance moisture meter. Tiitta et al. (1999) studied an electrical impedance frequency spectrum (20 Hz to 1 MHz) to measure the absorption and desorption transverse MC gradient by employing parallel-plate single-sided capacitive and conductive electrodes with similar results. Wilson (1999) found that in industrial conditions with timber stored under shelter, a capacitance-type meter performed better than three resistance-type meters.

Recently, near-infrared (NIR) spectroscopy has become the state-of-the-art technique for qualitative and quantitative analysis of agricultural materials. The absorption of light in the NIR region gives a spectrum that corresponds to specific vibrational modes and that is unique to each molecular structure examined. These vibrations in wood concern hydrogen groups with heteroatoms (C–H, O–H, etc.) and provide a wealth of information without a priori knowledge of either the spectral data or the chemical composition of the test material. NIR spectroscopy has been shown to be effective, especially in measuring MC, due to the strong absorbance of water in the spectrum (Windham and Barton 1988). It has been used to detect multiple traits of chemical, physical, mechanical and anatomical properties of wood materials (Watanabe et al. 2012; Tsuchikawa and Kobori 2015; Karttunen et al. 2008; Xu et al. 2011; Cooper et al. 2011). Defo et al. (2007) evaluated the effect of grain orientation on predicting MC and basic density in red oak (*Quercus* spp.); the spectra collected from the cross-sectional and radial surfaces provided better predictions than those collected from tangential surfaces. Recently, Kobori et al. (2015) developed an online NIR instrument to scan the length of lumber samples providing readings of sufficient accuracy to predict MC and MOE. Many calibration methods have been developed to analyze

spectrum data to achieve a high predictive accuracy (Dahlen et al. 2017; Savitzky and Golay 1964; Rantanen et al. 2001).

As described above, various researchers have mentioned the potential of capacitance sensors in combination with the NIR technique to estimate the MC of wood; however, their practical application in the wood industry is still somewhat restricted because of the limitation of the measured area and the measured depth from the material's surface. NIR spectroscopy is an efficient technique to predict MC, but spectral data are very large and the analytical process is quite complex. Most capacitance sensors will perform well under ideal conditions, but the accuracy changes as MC is below fiber saturation point. In this study, the results from the full range of MC from the green to air-dried state and the range from fiber saturation point to air-dried state were evaluated. Generally, variations in species and wood samples will affect meter readings and the interpretation of NIR spectra, including MC, thickness, density, grain direction and chemical constituents. In a previous study (Tham et al. 2018), the MC of many wood species was evaluated using a combination of capacitance sensor and NIR spectrophotometer on thin samples (02, 06 and 12 mm thickness) with good results. However, since problems remain for predictability for thicker samples, the first goal in this research was to investigate these techniques for thicker timber samples (100 mm thickness), in Japanese cedar (*Cryptomeria japonica*) and Japanese cypress (*Chamaecyparis obtusa*). The second goal was to develop novel predictive models by combining capacitance data and the NIR absorbance data at two informative wavelengths.

## Materials and methods

### Materials

Four logs (dimensions of  $100 \times 100 \text{ mm}^2$  in cross section and 2000 mm in length) of Japanese cedar and Japanese cypress were cut from the Toyota forest, southeast Japan. All logs were covered by plastic nylon to prevent water loss by evaporation; then, the experimental samples with the cubical dimensions of 100 mm were cut from these logs. The sample surfaces were prepared by cleaning and smoothing by using an automated single-sided planing machine. The experimental process was implemented in the controlled environmental room ( $20 \text{ }^\circ\text{C}$  and  $65\% \pm 5\%$  relative humidity). The capacitance and NIR spectra were measured on the cross section and tangential section of the samples. Sample weight, capacitance and NIR absorbance were measured every 4 h from the green state to the air-dried state; outside the experimental time, each sample was put in a nylon bag to limit the change of moisture in the samples. The capacitance and spectra were collected at three positions on each section of each sample. The data were collected from 20 samples of each species with 46 measurements until the moisture of the samples reached the air-dried state; it took approximately 2.5 months. To determine the reference MC, the small specimens were cut from the experiment samples with the dimensions of  $100 \times 50 \times 10 \text{ mm}^3$ . Then, the weights were measured and small samples were dried at  $103 \pm 20 \text{ }^\circ\text{C}$  for 48 h in the oven.

MC and density of experiment samples are provided in Table 1.

### Capacitance and NIR spectroscopy measurement

A high-frequency capacitance device (electrical moisture meter HM-530, Kett Electric Laboratory, Tokyo, Japan, Fig. 1a) set at a frequency of 20 MHz was used for capacitance measurement. Capacitance was measured at three positions on each section and then averaged for the whole sample. The equation below represents the capacitance of wood:

$$C_p = \varepsilon * K \quad (1)$$

where  $\varepsilon$  is the dielectric constant of wood containing moisture,  $K$  is the constant determined by measurement of the section shape, and  $C_p$  is the capacitance of the sample (pF).

A portable NIR spectrophotometer (MicroNIR™ OnSite, © 2015, VIAVI Solutions Inc., USA, Fig. 1b) in reflectance mode was used for the acquisition of the wood sample spectra using two integrated vacuum tungsten lamps; sample working plane 0–15 mm from window, 3 mm optimal distance; pixel-to-pixel interval 6 nm; input aperture dimensions 2.5 × 3.0 mm over a 908–1676-nm wavelength range with 256 scans; and an integration time of 7200  $\mu$ s. NIR spectra were measured at three positions on each section, and the mean was calculated for each section and the whole sample. NIR absorbance was calculated using the following equation:

$$A = -\log \left[ \frac{I}{I_0} \right] \quad (2)$$

where  $A$  is the NIR absorbance,  $I_0$  is the reflected light intensity from 99% diffuse reflectance panel, and  $I$  is the intensity of the light reflected from the wood samples.

Because the molar absorbance coefficient of the bands observed in the NIR region is small, it is necessary to accumulate and average the spectra for one measurement. The signal-to-noise ( $S/N$ ) ratio is a critical parameter for a high-quality spectrum, so increasing the signal level will also improve the signal-to-noise ratio and the measurement quality. The best number of scans,  $n=256$ , was tested and chosen. Another way to improve the predictive capability is to use preprocessing methods. Smoothing (Savitzky–Golay smoothing and derivatives), scattering correction (standard normal variate) and multiplicative scatter correction have been widely used to remove noise and unwanted signal. However, some preprocessing methods yielded little improvement in the performance of the results compared to using the original spectra data. Therefore, this study used the original spectra for the analysis. To reduce the noise effects of the capacitance device prior to carrying out the experiment, some input parameters were set up for the device, such as the specific gravity of the wood species and sample thickness and device temperature. In this study, the calibrations for capacitance sensor were carried out for Japanese cedar and Japanese cypress: thickness correction value with the dial of 40 mm because of the sample thickness being greater 40 mm and temperature correction value of 20 °C.

**Table 1** Density and moisture content of wood samples from the green to air-dried state

Wood species	Sample number	Air-dried density (g/cm <sup>3</sup> )	Oven-dried density (g/cm <sup>3</sup> )		Moisture content (%)		Density (g/cm <sup>3</sup> )			
			Max	Min	Mean	Max	Min	Max	Min	Mean
Japanese cedar	20	0.41	0.40	0.32	0.35	126.61	13.79	0.78	0.38	0.55
Japanese cypress	20	0.48	0.47	0.40	0.43	29.22	9.79	0.59	0.45	0.51

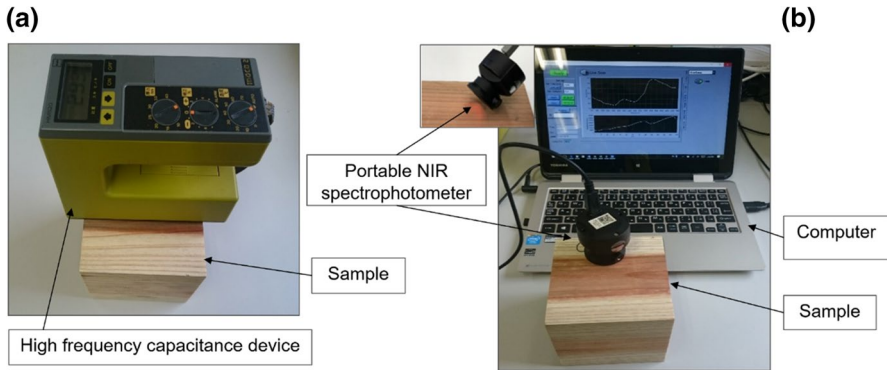


**Fig. 1** High-frequency capacitance device and portable NIR spectrophotometer

## Data analysis

The data were collected according to the flowchart shown in Fig. 2.

MATLAB software (Matlab R2016b; Math Works, Inc., USA) was used for the data analysis. The choice of an appropriate calibration method is very important as it affects the predictive performance. In this study, three calibration methods were studied: Capacitance-MLR, NIR-PLS and Capacitance+NIR-MLR, to select the best method on the basis of the performance of the output parameters. In all three calibrations, the leave-one-out was used in cross-validation to build and test the predictive models. A model is usually given a dataset of known data on which training

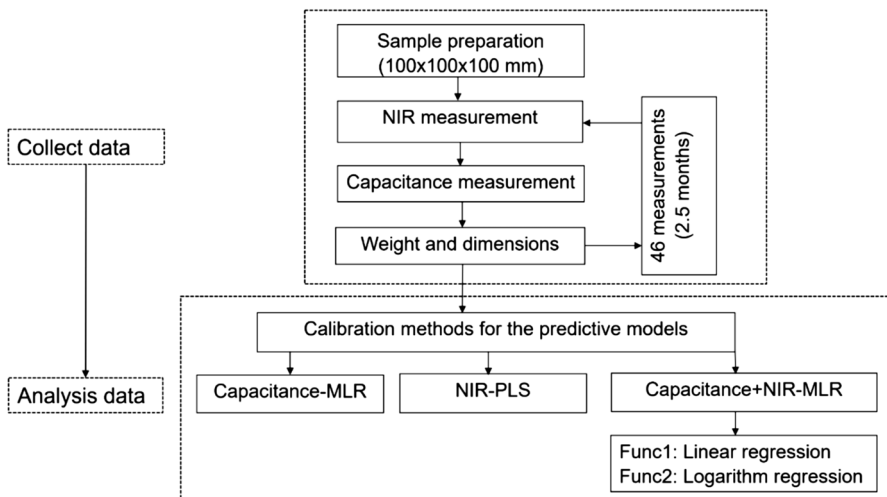


**Fig. 2** Experimental process and analysis methods for estimation of moisture content of timber. *MLR* multiple linear regression, *PLS* partial least square, *NIR* near-infrared spectroscopy, *Func1* and *Func2*: function 1 and function 2

is run (called training dataset or calibration dataset) and a dataset of unknown data against which the model is tested (called the validation dataset or testing set). The goal of cross-validation is to test the model's ability to predict new data. One round of cross-validation involves dividing the original samples into a calibration and a validation set. In this study, 'leave-one-out cross-validation (LOOCV)' was used with  $(n - 1)$  samples for the dataset in calibration ( $n$ : observed samples) and the one remaining sample used for the validation test.

Using MATLAB software,  $n$  rounds of cross-validation were repeated, and the best models were chosen corresponding to the lowest residual in cross-validation.

Fiber saturation point (FSP) is one of the important points which affect significantly the wood processing. FSP is the moisture point of wood when cell walls are completely saturated, and the moisture is started to transfer from cell wall into the cavities of the cells. FSP is not usually defined with any mathematical exactness (Babiak 1995), since it depends on the measurement technique, species, temperature, etc. The fiber saturation point varies depending on the wood species (e.g., oak, ash: 22–24%; pine, larch, Douglas-fir: 26–28%; fir, spruce: 30–34%) (Dietsch et al. 2015). The results were analyzed in two ranges of MC: 1—[Green to FSP] and 2—[FSP to air-dried state]. In this study, the FSP was determined with cedar species being 24.04% and cypress species being 22.17%.

*Capacitance-MLR* The models employed only the capacitance of wood under multiple linear regression. The relationship between the MC and the capacitance is a linear regression represented by the function below:

$$MC = A * C_p + B \quad (3)$$

where  $MC$  is the predicted moisture content (%),  $A$  is the regression coefficient,  $B$  is the intercept, and  $C_p$  is the capacitance of wood.

*NIR-PLS* The models used only NIR data under partial linear regression. The optimum number of PLS components (latent variable, LV) was determined by minimizing the residual between predicted values and observed values. Calibration and cross-validation were evaluated by various criteria, such as coefficient of determination for calibration ( $R_{cal}^2$ ) and for cross-validation ( $R_{val}^2$ ) between the predicted and the measured values; standard error of calibration (SEC) and prediction (SEP); root-mean-square error of calibration (RMSEC) and cross-validation (RMSECV). The ratio of performance to deviation (RPD) is the ratio between the standard deviation of the measured MC data and RMSECV for calibration ( $RPD_{cal}$ ) and cross-validation ( $RPD_{val}$ ). The models of PLS were calculated using the functions below:

$$Y = C * X + E \quad (4)$$

$$C = (X^T X)^{-1} * X^T * Y \quad (5)$$

where  $X$  is the spectra matrix,  $Y$  is the independent variate,  $C$  is the coefficient constant,  $E$  is the intercept,  $X^T$  is the inverted matrix of  $X$ , and T denotes transpose.

*Capacitance + NIR-MLR* The models operated the capacitance and NIR absorbance at two informative wavelengths under multiple linear regression. In the NIR-PLS calibration, the full wavelength spectrum was employed. However, this is time-consuming and computationally complex, and there is a high overlap

in the spectra. To overcome these problems, a new method, Capacitance + NIR-MLR, was developed employing only selected wavelengths for the models. Some of the advantages include the decreased noise, faster operation and tighter focus on regions of maximum information. This procedure called “stepwise regression” was used to determine the optimal spectral “region” (or wavelength). The primary wavelength (or region) may require argumentation from other wavelengths (regions) to correct for nonlinearities or interference, and to achieve good results, two or more wavelengths are required. In this study, the minimum requirement of two wavelengths was met for building the functions. As an ideal design, it is suggested that the new device is composed of a capacitance sensor, two LEDs making NIR light at two wavelengths, photodetectors and sensors.

To determine the two optimum wavelengths for NIR absorbance, a stepwise selection is applied over all wavelengths, and the two wavelengths which yield the lowest residual were chosen. After selecting the two optimum wavelengths, the predicted models were built using linear and nonlinear regressions and compared to choose the most suitable one. These two regressions were chosen because of the simplicity of the linear function (MLR) and of the ability to cope with a nonlinear function. Nonlinear algorithms can produce better results than traditional linear methods, especially when used together with large NIR spectral libraries (Pérez-Marín et al. 2012). The derivation of the mathematical expressions is shown in the two following functions:

$$\text{Func1: MC} = A_1 * \text{Abs}(\lambda_1) + A_2 * \text{Abs}(\lambda_2) + A_3 * C_p + D \quad (6)$$

$$\text{Func2: MC} = A_1 * (\text{Abs}(\lambda_1) - \text{Abs}(\lambda_2))^{A_2} * C_p + D \quad (7)$$

where  $C_p$  is the capacitance of wood;  $\text{Abs}(\lambda_1)$  and  $\text{Abs}(\lambda_2)$  are NIR absorbance at two wavelengths;  $A_1$ ,  $A_2$  and  $A_3$  represent regression coefficients;  $D$  is the intercept; MC is the predicted moisture content; and Func1 and Func2 represent function 1 using multiple linear regression and function 2 using the logarithmic regression for the models in Capacitance + NIR-MLR calibration. Statistical analysis was used to compare the accuracy and performance of the two functions.

1. Confidence interval for accuracy: For large test sets ( $N > 30$ ), the accuracy (acc) has a normal distribution with mean  $p$  and variance  $p(1-p)/N$ . Confidence level 95%,  $Z_{\alpha/2} = 1.96$ .

Confidence interval for  $p$  is:

$$p \left( Z_{\frac{\alpha}{2}} < \frac{\text{acc} - p}{\sqrt{p(1-p)/N}} < Z_{\frac{\alpha}{2}} \right) = 1 - \alpha. \quad (8)$$

2. Analysis of variance was conducted using the  $\alpha = 0.05$  level to determine whether the model performance was different between models.

If the interval contains 0, the different performance of the two models may not be statistically analytically significant.



The performance of the most robust methods was evaluated in terms of the LV, SEC, SEP, RPD and  $R^2$  for the calibration and validation as well as the stability of the models. Then, the predictive models are shown under Func1 and Func2.

## Results and discussion

### Results for Capacitance-MLR calibration

The results of  $R^2_{\text{val}}$  and  $\text{RPD}_{\text{val}}$  of three calibrations in [Green to FSP] were quite good and much higher than the results obtained in [FSP to air-dried state]. In detail, in Table 2, the first calibration, Capacitance-MLR, in [Green to FSP] demonstrated good predictive ability on cross section and on the whole sample, except for the case of tangential section. The second and third calibrations, NIR-PLS and Capacitance+NIR-MLR, were better than the first one on three sections with  $R^2_{\text{val}} > 0.81$ . In particular, Capacitance+NIR-MLR showed the best calibration with the highest accuracy  $R^2_{\text{val}}$  and RPD, and the lowest SEP. In Table 3, although the coefficient of determination in [FSP to air-dried state] was lower than in [Green to FSP], the standard error of prediction (SEP) was lower ( $< 2.26$ ). It means the difference between the actual or real values and the predicted values is smaller than in the first MC range. This criterion is also very significant in the real manufacturing.

Comparing the two MC ranges in Table 2 with Table 3, the performance in [Green to FSP] was better than the results in [FSP to air-dried state]. The reason may be due to the range of MC; as MC of samples decreases, both capacitance of wood and NIR absorbance decrease. However, the gradient of MC from the score to the surface of the samples in [Green to FSP] is smaller than in [FSP to air-dried state]; therefore, the reading value of the devices is similar to the real MC of the whole sample. In this study, the samples are thick (100 mm thickness); as MC of samples reaches near the air-dried state, the difference of MC between the score and surface of samples is higher. The reading MC value on the surface might not present the MC of the whole samples, making the accuracy of prediction to decrease.

However, the predictive ability varied not only depending on the measured section of the samples but also on wood species. Figure 3 illustrates the relationship between capacitance and actual MC of two Japanese species for each section type. The capacitance on the cross section was higher than on the tangential section in both species (Fig. 3a, b). This anisotropy can be explained by the difference in dielectric properties along and across the grain of the wood due to the differences in the arrangement of the cell wall and lumen. Since the structures on the cross section (ray parenchyma and tracheid) are mainly aligned with the longitudinal direction of the trunk, the cross section loses much more water by evaporation from the green state to the air-dried state. Hence, the capacitance readings for the cross section were higher than for the tangential section. Kabir et al. (1998) reported that MC of rubber wood affected dielectric properties considerably at both low and microwave frequencies. Both the dielectric constant and dielectric loss factor increase as MC increases from 0 to around 30% and increase slightly for both parallel and perpendicular to grain directions at low frequency. Nursultanov et al. (2017) reported that

**Table 2** Summary of the results of three calibrations on the different sections for predicting MC of timber in [Green to FSP]

Calibration method	Section	Prediction of MC from green to FSP (%)									
		LV	$R^2_{\text{cal}}$	$R^2_{\text{val}}$	SEC (%)	SEP (%)	$\lambda_1$ (nm)	$\lambda_2$ (nm)	RPDcal	RPDval	
Capacitance-MLR	All		0.92	0.92	7.27	7.29			3.55	3.54	
NIR-PLS	All	4	0.91	0.91	7.67	7.75			3.37	3.33	
Capacitance+NIR-MLR (Func1)	All		0.95	0.95	5.83	5.86	1224	1236	4.43	4.41	
Capacitance-MLR	Tangential		0.69	0.68	14.50	14.53			1.78	1.78	
NIR-PLS	Tangential	8	0.82	0.81	10.98	11.24			2.35	2.30	
Capacitance+NIR-MLR (Func1)	Tangential		0.82	0.82	11.04	11.09	1162	1230	2.34	2.33	
Capacitance-MLR	Cross		0.94	0.94	6.11	6.13			4.23	4.22	
NIR-PLS	Cross	4	0.92	0.92	7.20	7.26			3.59	3.56	
Capacitance+NIR-MLR (Func1)	Cross		0.96	0.96	5.17	5.20	1230	1236	4.99	4.97	

**Table 3** Summary of the results of three calibrations on the different sections for predicting MC of timber in [FSP to air-dried state]

Calibration method	Section	Prediction of MC in [FSP to air-dried state] (%)									
		LV	$R^2_{cal}$	$R^2_{val}$	SEC (%)	SEP (%)	$\lambda_1$ (nm)	$\lambda_2$ (nm)	RPD <sub>cal</sub>	RPD <sub>val</sub>	
Capacitance-MLR	All		0.45	0.45	2.18	2.19			1.35	1.34	
NIR-PLS	All	13	0.79	0.77	1.35	1.40			2.18	2.09	
Capacitance + NIR-MLR (Func1)	All		0.70	0.70	1.61	1.62	1168	1212	1.83	1.82	
Capacitance-MLR	Tangential		0.41	0.41	2.25	2.26			1.31	1.30	
NIR-PLS	Tangential	15	0.76	0.73	1.43	1.52			2.05	1.93	
Capacitance + NIR-MLR (Func1)	Tangential		0.64	0.63	1.77	1.78	1459	1472	1.66	1.65	
Capacitance-MLR	Cross		0.43	0.43	2.22	2.23			1.32	1.32	
NIR-PLS	Cross	10	0.76	0.75	1.41	1.47			2.08	2.00	
Capacitance + NIR-MLR (Func1)	Cross		0.72	0.72	1.54	1.56	1013	1038	1.90	1.89	

Capacitance-MLR, NIR-PLS, Capacitance + NIR-MLR: three calibrations in analysis process

Func1 Function 1 in Capacitance + NIR-MLR calibration, LV latent variable,  $R^2_{cal}$  and  $R^2_{val}$  coefficients of determination in calibration and validation, SEC and SEP standard errors of calibration and prediction,  $\lambda_1$  and  $\lambda_2$  wavelengths, RPD<sub>cal</sub> and RPD<sub>val</sub> ratios of performance to deviation in calibration and validation, FSP fiber saturation point of wood

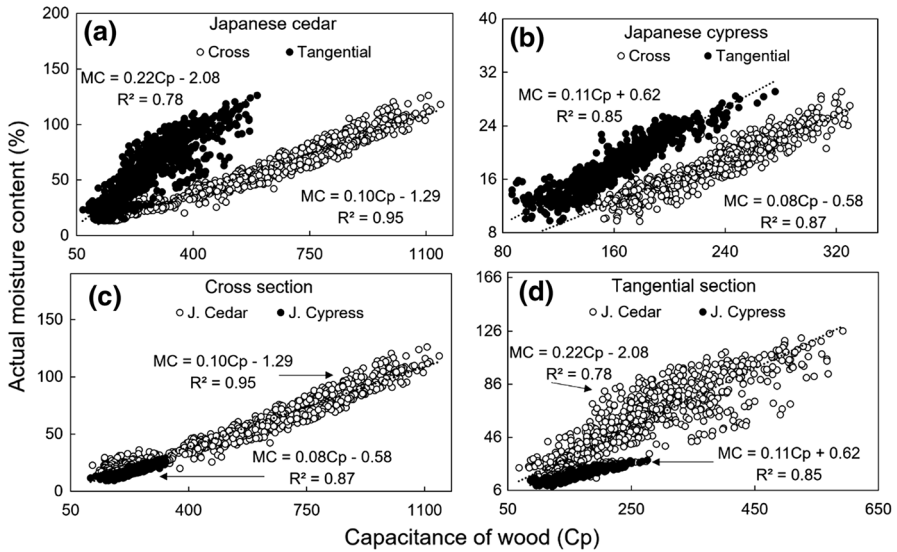


**Fig. 3** Relationship between actual moisture content and capacitance from two species and two sections. Vertical axis: actual MC; horizontal axis: capacitance of wood;  $R^2$ : coefficient of determination; **a**, **b**: results for Japanese cedar and cypress on the cross and tangential sections; **c**, **d**: results for cross and tangential sections for each species (J. cedar and J. cypress: Japanese cedar and cypress with oven-dried densities of 0.35 and 0.43 g/cm<sup>3</sup>)

the electrical conductivity in green *Pinus radiata* in the longitudinal direction was around 20 times higher than in the tangential direction, and 10 times higher than in the radial direction. In this study, the  $R^2$  value on the cross section was higher than on the tangential section for both species (cross section of 0.95 and tangential section of 0.78 for Japanese cedar (Fig. 3a), with a similar tendency for Japanese cypress (Fig. 3b).

Figure 3c, d illustrates the influence of density on the prediction of MC. The slopes of the linear regression were calculated from the relationship between capacitance and MC. The linear regression slopes in the models for Japanese cedar were higher than for Japanese cypress in both section types, especially on the tangential section, with the values of 0.22 and 0.11, respectively (Fig. 3d). The oven-dried densities of the two species were similar, but the ranges of MC from the green state to air-dried state varied greatly (Table 1), the range for Japanese cedar being 126.61–13.79% and that for Japanese cypress being 29.22–9.79%. Japanese cedar samples had both heartwood and sapwood in a quite equal proportion, while the Japanese cypress samples consisted mainly of heartwood on both the cross and tangential sections. The MC in sapwood is usually higher than in heartwood in cypress species (Haslett et al. 1985). The density was one factor accounting for the difference between the linear regression slopes of the two species.

In a previous experiment (Tham et al. 2018), the capacitance of 14 wood species was investigated for the thin samples with three kinds of thicknesses (2, 6 and 12 mm thickness) for 14 wood species (*Kalopanax septemlobus*, *Cercidiphyllum japonicum*,

*Cryptomeria japonica*, *Chamaecyparis obtuse*, *Hevea brasiliensis*, *Eusideroxylon zwageri*, *Agathis alba* Foxw, *Paulownia tomentosa*, *Fraxinus mandshurica*, *Fagus sylvatica*, *Triplochiton scleroxylon*, *Araucaria angustifolia*, *Liriodendron tulipifera* and *Thuja plicata*). This current research studied two wood species: Japanese cedar (*Cryptomeria japonica*) and Japanese cypress (*Chamaecyparis obtuse*). In the analytical section of the relationship between the capacitance, MC and density of wood, the results of the current study and the previous study (Tham et al. 2018) are used. We will have the data of four thicknesses for analysis as shown in Fig. 4.

For the data of one species of each kind of thickness, the relationship between capacitance of wood and MC was built by using the linear regression in Eq. (4). The slopes of capacitance and MC (designated “A”) showed the relationship between the capacitance and the predicted variant (MC). The density, thickness and MC of the samples all affect the A value. Therefore, A was used to describe the relationship between capacitance and MC in fourteen wood species; the bigger the slope A, the stronger the dependence of capacitance on density of wood species. One species possesses a specific oven-dried density, meaning one species has one specific slope A at one oven-dried density. For example, in Fig. 3c for the cross section, there were two A values for the two species at two oven-dried densities: Japanese cedar ( $0.35 \text{ g/cm}^3$ ) at the slope A of 0.10 and Japanese cypress ( $0.43 \text{ g/cm}^3$ ) at the slope A of 0.08.

Figure 4 shows the relationship between the slope A and the oven-dried density at four kinds of thicknesses. This relationship was calculated following the equation:

$$y = a * \ln(x) + b \quad (9)$$

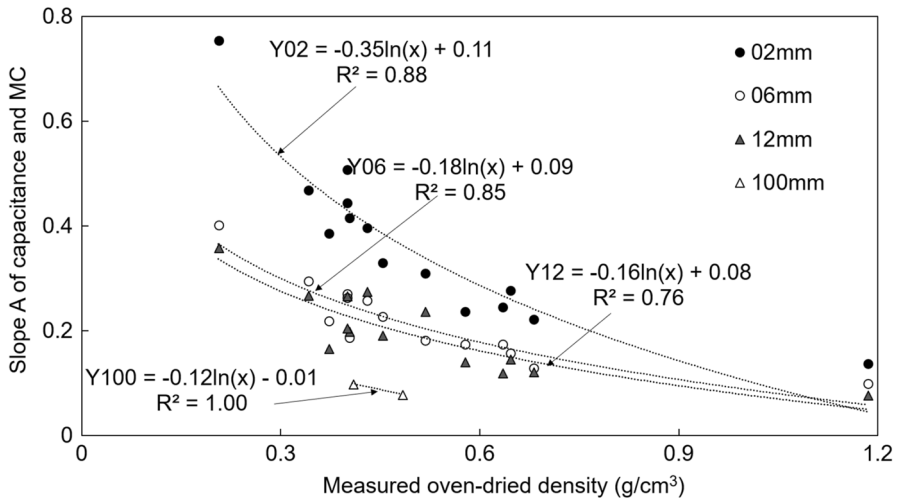


**Fig. 4** Relationship between the slope A of capacitance and MC with oven-dried density for four kinds of thicknesses (y<sub>2</sub>, y<sub>6</sub>, y<sub>12</sub> and y<sub>100</sub>: the equations for 2, 6, 12 and 100 mm thickness; y: the slope A of capacitance and MC; x: the measured oven-dried density; 14 species for each kind of 2, 6, 12 mm thicknesses and 2 species for 100-mm-thick samples, one species corresponding to one oven-dried density and assigned one point in the figure)

where  $x$  is the oven-dried density ( $\text{g/cm}^3$ ),  $y$  is the slope  $A$  of capacitance and MC,  $a$  is the coefficient, and  $b$  is the intercept.

As shown in Fig. 4, the  $A$  values changed according to the sample thickness and oven-dried density.  $A$  decreased as the thickness increased; for example, at an oven-dried density of  $0.21 \text{ g/cm}^3$ , the values for slope  $A$  were 0.76 for the 2-mm sample, 0.40 for the 6-mm sample and 0.36 for the 12-mm sample. The same trend was observed for each sample thickness, with  $A$  values declining as the oven-dried density increased; for example, 2-mm samples showed slope  $A$  values of 0.47 at  $0.34 \text{ g/cm}^3$  and 0.14 at  $1.18 \text{ g/cm}^3$ . These results indicate a strong relationship between slope  $A$  and oven-dried density, the thinner samples with low density showing the stronger correlation. Finally, the logarithm function expressed the most suitable regression for illustrating the relationship between capacitance, MC and density.

The slopes of the linear regression were calculated from the relationship between capacitance and MC for cedar and cypress species (Fig. 3); each species with its density value corresponds to one slope's value. Therefore, different densities had different predictions of MC and different slopes had different coefficients of determination ( $R^2$ ) as shown in Fig. 3 (Point 1).

The relationship between slopes and oven-dried density was in four groups of thickness as shown in Fig. 4. It can be clearly seen the difference in the four logarithm lines in four kinds of thickness (2, 6, 12 and 100 mm thickness). Thinner sample had higher slope than thicker sample of the same species, for example, *Paulownia tomentosa* with oven-dried density of  $0.25 \text{ g/cm}^3$  at three levels of thickness following three slope values in Fig. 4 (Point 2).

Combining Point 1 and Point 2, the relationship between capacitance, MC and density of wood can be shown by the slope parameter. The slopes varied in thickness and density of wood, and the slopes also affected the predictable accuracy of MC.

## Results for NIR-PLS calibration

NIR-PLS calibration yielded high accuracy results (Tables 2, 3) in both MC ranges of [Green to FSP] and [FSP to air-dried state]. For example, as given in Table 2, the  $R^2_{\text{val}}$  values were 0.81, 0.91 and 0.92, and the  $\text{RPD}_{\text{val}}$  values were 2.30, 3.33 and 3.56 for the tangential section, whole sample and cross section, respectively. As given in Table 3, the estimation was lower, with  $R^2_{\text{val}}$  values from 0.73 to 0.77. SEP and RPD values also decreased when MC was from FSP to air-dried state. The  $R^2_{\text{val}}$  of cross-validation for the prediction of MC in [Green to FSP] was higher than in [FSP to air-dried state]. This is due to the gradients of water between the score and surface of the samples. When samples dry in room condition, this gradient is not so large for the wood in [Green to FSP]; it maybe has the better prediction of MC than in [FSP to air-dried state]. On the other hand, the results of NIR-PLS calibration in [FSP to air-dried state] were better than other calibrations with the highest  $R^2_{\text{val}}$  (0.73 to 0.77) and  $\text{RPD}_{\text{val}}$  ( $\geq 2.00$ ) and the lowest SEP ( $\leq 1.52$ ), although the number of latent variables (LVs) was quite high (from 10 to 15) compared to the results in [Green to FSP]. The NIR spectrophotometer can estimate the MC of timber effectively by using the full range of wavelengths from 908 nm to 2676 nm in both MC ranges.

As given in Table 2, the results achieved with this calibration were higher than those obtained in the research by Hein et al. (2009), where *Eucalyptus urophylla* and *Eucalyptus grandis* were evaluated using original spectral data from cross-validation models, yielding an  $R^2_{\text{val}}$  of 0.74 and an  $\text{RPD}_{\text{val}}$  value of 2.00. The results in the present study for the cross section ( $R^2_{\text{val}}=0.92$ ,  $\text{RPD}_{\text{val}}=3.56$ ) were higher than for the tangential section ( $R^2_{\text{val}}=0.81$ ;  $\text{RPD}_{\text{val}}=2.30$ ). The results achieved in the calibrated models using combined mean data from cross and tangential sections for the whole samples also provided very good estimates ( $R^2_{\text{val}}=0.91$ ;  $\text{RPD}_{\text{val}}=3.33$ ). On the other hand, the predictions on the cross section in both MC ranges were higher than those from tangential section. Because the cross section consists of many longitudinal tracheids and ray parenchyma cells, light might penetrate deeper into the cross section than into the tangential section, leading to less reflectance (Tsuchikawa et al. 1996; Schimleck et al. 2003). Both cross and tangential sections absorbed NIR light in the same bands, but in differing intensities (Defo et al. 2007). As a result, the cross section provided more comprehensive information about the materials. Yang et al. (2015) suggested that the NIR models based on spectra from three sections provided the highest accuracy compared to models involving cross sections.

### Results for Capacitance + NIR-MLR calibration

Each NIR spectrum arises from a wide range of wavelengths (908–1676 nm) and therefore yields a large volume of data. To deal with such information-rich datasets, considerable efforts have been directed toward the following problems: regression analysis (calibration method), wavelength selection and model improvement. In case of Capacitance + NIR-MLR, the calibration method and wavelength selection were chosen with the aims of improving accuracy and removing uninformative wavelengths. The present method combined capacitance with NIR absorbance at two optimal wavelengths, yielding improved results for all sections (Table 2). Similar to Capacitance-MLR and NIR-PLS calibrations, the results from the cross sections were better than those from the tangential sections due to the anisotropic nature of the wood. The capacitance and NIR absorbance were higher in the cross section than in the tangential section because of the cross section of cut tracheids versus the vertical walls of the tracheids. The tangential plane exhibits the grain of the wood, as it is the view parallel to the wall of wood cells in the tree, so it is quite smooth and uniform. Another reason is both species have the distinct earlywood and latewood (springwood and summerwood) on the cross section, with the much higher ratio of earlywood than latewood in annual growth rings. Earlywood consists of the larger cells with the thin-walled tracheids. Therefore, water evaporated from the cross sections was higher than that from the tangential sections when the samples were dried gradually, leading to their higher capacitance readings. In addition, the NIR light was dispersed and absorbed onto the cross-sectional surface much more than onto the tangential surface. Therefore, the cross section provided more information and achieved the better estimation of MC, for example, in Table 2,  $R^2_{\text{val}}$  being 0.82, 0.95 and 0.96, and the  $\text{RPD}_{\text{val}}$  being 2.33, 4.41 and 4.97 for the tangential section, whole sample, and cross section, respectively, in Capacitance + NIR-MLR calibration. In

Table 3, the best calibration is NIR-PLS calibration. The NIR spectroscopy has high potential prediction for MC range from air-dried state to the green, while Capacitance + NIR-MLR calibration has higher prediction in [Green to FSP]; the performance decreases in [FSP to air-dried state].

Capacitance + NIR-MLR calibration shows as a good approach with the high prediction in [Green to FSP]; NIR-PLS is the good calibration in [FSP to air-dried state]. The capacitance directly relates to the electrical properties of wood, whereas NIR spectroscopy provides information about the chemical bonds and molecular structure; therefore, combining the two measurement methods limits some of the drawbacks of each device, as well as improves the data necessary for the accurate prediction of MC. NIR spectroscopy has a good potential for prediction in both ranges of MC. The results for the two species in [Green to FSP] had higher  $R^2_{\text{val}}$  and RPD and SEP than the results in [FSP to air-dried state].

It was continued to build the predicted models in Capacitance + NIR-MLR calibration. Models were built from two kinds of regressions: multiple linear regression and logarithmic regression in Eqs. (7) and (8). Firstly, it was attempted to use the simplest regression, multiple linear regression, for three variates (capacitance of wood and NIR absorbance at two wavelengths). Besides, from the results of Capacitance-MLR calibration, the relationship between the slopes  $A$  and densities was discussed and indicated that the logarithm transformation was the best fit (Fig. 4). For these reasons, in this study, two kinds of regression (multiple linear and logarithmic regression) were used for building the models. The details of the models for estimating the MC of wood using two equations on the different sections are shown in Tables 4 and 5 according to the ranges in [Green to FSP] and [FSP to air-dried state].

As given in Table 4, in [Green to FSP], both function 1 and function 2 produced quite similar results and very high predictive ability, with  $R^2_{\text{val}}$  ranging from 0.87 to 0.96. The logarithmic regression Func2 used three regression coefficients, while the multiple linear regression Func1 used four. The coefficients of determination  $R^2$  in Func2 were a little higher than in Func1, but the standard error of prediction SEP was also higher. From the results of Tables 4 and 5, the  $R^2$  values of Func1 and

**Table 4** Regression models and determination coefficients for predicting MC in [Green to FSP] under two regressions in Capacitance + NIR-MLR calibration

Function	Section	Algorithm for prediction of MC of timbers	$R^2_{\text{val}}$	SEP
Func1	All	$MC = -14433.60 * \text{Abs}(1224) + 14466.74 * \text{Abs}(1236) + 0.10 * C_p + 91.49$	0.95	5.86
Func1	Cross	$MC = -8.75 * \text{Abs}(1230) + 53.12 * \text{Abs}(1236) + 0.20 * C_p - 12.21$	0.92	5.20
Func1	Tangential	$MC = 6304.02 * \text{Abs}(1162) + 6303.02 * \text{Abs}(1230) + 0.13 * C_p + 38.61$	0.82	11.09
Func2	All	$MC = 0.14 * (\text{Abs}(1162) - \text{Abs}(1186))^{-0.02} * C_p - 7.50$	0.95	7.81
Func2	Cross	$MC = 0.09 * (\text{Abs}(994) - \text{Abs}(1236))^{-0.02} * C_p - 4.05$	0.96	7.77
Func2	Tangential	$MC = 0.22 * (\text{Abs}(1242) - \text{Abs}(1286))^{-0.01} * C_p - 0.99$	0.87	14.32



**Table 5** Regression models and determination coefficients for predicting MC in [FSP to air-dried state] under two regressions in Capacitance + NIR-MLR calibration

Function	Section	Algorithm for prediction of MC of timbers	$R^2_{val}$	SEP
Func1	All	$MC = 510.58 * Abs(1168) - 492.12 * Abs(976) + 0.07 * C_p + 10.58$	0.70	1.62
Func1	Cross	$MC = 3133 * Abs(1012) - 3107.04 * Abs(1038) + 0.04 * C_p + 4.24$	0.72	1.56
Func1	Tangential	$MC = 555.65 * Abs(1460) - 542.37 * Abs(1472) + 0.08 * C_p - 2.88$	0.63	1.78
Func2	All	$MC = 0.06 * (Abs(1174) - Abs(1242))^{-0.02} * C_p + 6.09$	0.70	2.29
Func2	Cross	$MC = 0.04 * (Abs(964) - Abs(988))^{-0.02} * C_p + 7.09$	0.70	2.38
Func2	Tangential	$MC = 0.06 * (Abs(1460) - Abs(1484))^{-0.02} * C_p + 6.42$	0.63	2.36

$Abs(\lambda)$  NIR absorbance at wavelength  $\lambda$ ,  $C_p$ : capacitance of wood,  $MC$  moisture content,  $R^2_{val}$  coefficient of determination in cross-validation, *Func1* and *Func2* the predicted models using multiple linear and logarithmic regressions in Capacitance + NIR-MLR calibration

**Table 6** Comparison between Func1 and Func2 regarding accuracy and performance in [Green to FSP]

Capacitance + NIR-MLR	Section	Confidence interval for accuracy		Comparing performance of models
		$P_{lower}$ (%)	$P_{upper}$ (%)	
Func1	All	0.934	0.963	$d_t = \pm 0.203$ , the difference may not be statistically significant
Func2	All	0.934	0.963	
Func1	Tangential	0.793	0.844	$d_t = 0.05 \pm 0.034$ , the difference may be statistically significant
Func2	Tangential	0.846	0.891	
Func1	Cross	0.900	0.936	$d_t = 0.04 \pm 0.022$ , the difference may be statistically significant
Func2	Cross	0.945	0.971	

**Table 7** Comparison between Func1 and Func2 regarding accuracy and performance in [FSP to air-dried state]

Capacitance + NIR-MLR	Section	Confidence interval for accuracy		Comparing performance of models
		$P_{lower}$ (%)	$P_{upper}$ (%)	
Func1	All	0.668	0.731	$d_t = \pm 0.046$ , the difference may not be statistically significant
Func2	All	0.668	0.731	
Func1	Tangential	0.595	0.664	$d_t = \pm 0.048$ , the difference may not be statistically significant
Func2	Tangential	0.595	0.664	
Func1	Cross	0.687	0.751	$d_t = 0.02 \pm 0.045$ , the difference may not be statistically significant
Func2	Cross	0.668	0.731	

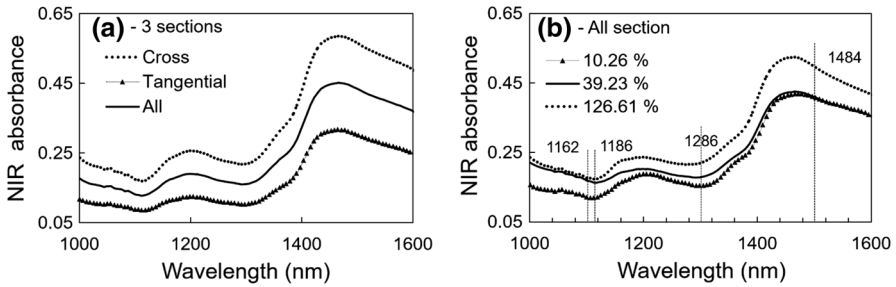


**Fig. 5** Original NIR spectra (a) on three different sections: cross, tangential and average for the whole sample (all), and NIR absorbance on all sections (b) at three levels of MC showing some of the selected wavelengths for the predictive models for Func1 and Func2 in Capacitance + NIR-MLR calibration

Func2 were close, but Func1 had lower SEP than Func2. In this case, the function 1 should be used for the predicted models.

On the other hand, the confidence interval for accuracy and the different performance between two functions are evaluated in Tables 6 and 7. As given in Table 6 with MC in [Green to FSP], the Func1 and Func2 had the similar confidence interval of accuracy. The confidence interval for accuracy of Func2 was a little higher on the cross and tangential sections, being equal on the tangential section with Func1. The performance of the two functions may be statistically significant on the cross and tangential sections, but it may not be statistically significant on all sections. As given in Table 7 with MC in [FSP to air-dried state], the confidence interval for accuracy of the two functions was similar, and their performance difference may not be statistically significant on all sections of samples.

The predictive models in Tables 4 and 5 employed NIR absorbance at only two wavelengths. Figure 5a illustrates the original spectrum of the wood samples on cross section, tangential section and mean values for the whole sample, while Fig. 5b describes the NIR absorbance for the whole sample at three levels of MC and some selected wavelengths used in the predicted models. The peaks in Fig. 5a indicate high absorption of NIR electromagnetic energy. The height and shape of the spectra are dependent on scattering of light. This scatter is affected by difference in reflectance nature of the sample surface, moisture concentration and the structures of sections. According to the principle of NIR reflectance spectroscopy, a beam of radiation is illuminated on the sample, penetrates a few millimeters, is diffused, and is then reflected back to the detector. Since the radiation penetrated and interacted with the sample, it carries absorption information and the representative spectra are returned as NIR absorption curves. Figure 5a shows that different sections had different light absorbances, the highest being for the cross section. One of the reasons is its special anatomical structure; therefore, the amount of water and OH bonding groups on the cross section are normally higher than on the tangential section when MC was drying from the green state. Figure 5b illustrates the NIR spectral curves at three levels of moisture, with some of the informative wavelengths used in the predicted models. The higher MC had the higher NIR absorbance because of the high amount of OH bonding groups. An NIR spectrum comprises many bands owing to

overtone and combination modes that are usually highly overlapping, and which often designate overly low absorption and more noise. Therefore, the two informative wavelengths are chosen with the goal of reducing the noise and improve the prediction in Capacitance+NIR-MLR calibration. Multivariate analysis has frequently been used to overcome this sensitivity problem (Jouan-Rimbaud et al. 1995; Jiang et al. 2002; Mehmood et al. 2012). Wavelengths corresponding to the lowest residual were selected for the models. In this study, the chosen wavelengths (Fig. 5b) used for the predicted models were mainly assigned to the OH group bonding in water, hemicellulose, cellulose in wood. Other studies have also proposed that the NIR spectra of wood vary with the sample MC; absorbance bands near  $7320\text{ cm}^{-1}$  (1366 nm),  $7160\text{ cm}^{-1}$  (1400 nm) and  $7000\text{ cm}^{-1}$  (1428 nm) were related to cellulose and water (Fujimoto et al. 2012). These specific bands can fluctuate because of slight baseline shifts with changes in MC, molecular structure between measured sections, and wood species. This baseline shift in bands related to the water and cellulose functional groups was observed in the present samples as they gradually dried from the green state to the air-dried state, and the OH group bonding also decreased. Capacitance+NIR-MLR calibration used NIR spectra in two wavelengths so that the scattering and overlapping phenomena would be reduced and the spectral interpretation would be more efficient. The wavelengths chosen in the models were different in the measured sections due to the differences in structure between the cross and tangential sections, which have differing MC gradients and light penetration depths from the surface.

## Conclusion

This study demonstrates a new nondestructive approach for predicting the MC of timbers from the green to the air-dried state by coordinating wood capacitance and NIR absorbance at two informative wavelengths. Such an approach is highly accurate and quicker and involves simpler analyses based on a much reduced dataset. This study employed MLR and PLS to build predictive models. Three calibrations were implemented from the data obtained by a capacitance sensor and NIR spectrophotometer, the data being processed individually or in combination. All calibrations achieved good results in [Green to FSP], yielding a high accuracy for coefficient of determinations in cross-validation, but the results in [FSP to air-dried state] had the smaller standard error of prediction. In both MC ranges and in all calibrations, the predictions on cross section were higher than on the tangential section because of the anatomical characteristics of wood material. A new method was studied as combining the data of capacitance and NIR absorbance at two informative wavelengths, and the predictive models were developed under two kinds of functions: multiple linear regression and logarithmic regression. This new calibration improved the accuracy in [Green to FSP], and NIR-PLS calibration was better in [FSP to air-dried state]. Depending on the MC ranges, the two functions (linear and nonlinear regressions) had a different performance in [Green to FSP], and the performance of these models may not be statistically significantly different in [FSP to air-dried state].

This research provides the basis for a new analytical method for estimating MC of timber, as well as for assessing other properties of wood and wood-based materials. It may be feasible to construct a new device, which is mainly composed of capacitance sensor, two LEDs (to make two wavelengths), photodetectors and sensors. It can be used for predicting MC of wood with on-site or online applications in the future.

**Acknowledgements** This research was partly supported by the Research and Development Studies for Application in Promoting New Policy of Agriculture, Forestry, and Fisheries, Japan [No. 22003].

## References

- Babiak MJ (1995) A contribution to the definition of the fiber saturation point. *J Wood Sci Technol* 29(3):217–226
- Cooper PA, Jeremic D, Radivojevic S, Ung YT, Leblon B (2011) Potential of near-infrared spectroscopy to characterize wood products. *Can J For Res* 41(11):2150–2157. <https://doi.org/10.1139/x11-088>
- Dahlen J, Diaz I, Schimleck L, Jones PD (2017) Near-infrared spectroscopy prediction of southern pine No. 2 lumber physical and mechanical properties. *Wood Sci Technol* 51(2):309–322
- Defo M, Taylor AM, Bond B (2007) Determination of moisture content and density of fresh-sawn red oak lumber by near infrared spectroscopy. *For Prod* 57(5):68–72
- Dietsch P, Franke S, Franke B, Gamper A, Winter S (2015) Methods to determine wood moisture content and their applicability in monitoring concepts. *J Civ Struct Health Monit* 5(2):115–127
- Fujimoto T, Kobori H, Tsuchikawa S (2012) Prediction of wood density independent of moisture conditions using near infrared spectroscopy. *Near Infrared Spectrosc* 25:353–359
- Haslett A, Williams D, Kininmonth J (1985) Drying of major cypress species grown in New Zealand. *N Z J For Sci* 15(3):370–383
- Hein PRG, Campos ACM, Trugilho PF, Lima JT, Chaix G (2009) Near infrared spectroscopy for estimating wood basic density. *Cerne, Lavras* 15(2):133–141
- Jiang JH, Berry RJ, Siesler HW, Ozaki Y (2002) Wavelength interval selection in multicomponent spectral analysis by moving window partial least-squares regression with applications to mid-infrared and near-infrared spectroscopic data. *Anal Chem* 74(14):3555–3565
- Jouan-Rimbaud D, Walczak B, Massart DL, Last IR, Prebble KA (1995) Comparison of multivariate methods based on latent vectors and methods based on wavelength selection for the analysis of near-infrared spectroscopic data. *Anal Chim Acta* 304(3):285–295
- Kabir MF, Daud WM, Khalid K, Sidek HAA (1998) Dielectric and ultrasonic properties of rubber wood. Effect of moisture content grain direction and frequency. *Holz Roh Werkst* 56:223–227
- Karttunen K, Leinonen A, Saren MP (2008) A survey of moisture distribution in two sets of Scots pine logs by NIR-spectroscopy. *Holzforschung* 62(4):435–440
- Kobori H, Inagaki T, Fujimoto T, Okura T, Tsuchikawa S (2015) Fast online NIR technique to predict MOE and moisture content of sawn lumber. *Holzforschung* 69(3):329–335
- Mehmood T, Liland KH, Snipen L, Sæbø S (2012) A review of variable selection methods in partial least squares regression. *Chemom Intell Lab Syst* 118:62–69
- Meyer L, Brischke C (2015) Fungal decay at different moisture levels of selected European-grown wood species. *Int Biodeterior Biodegrad* 103:23–29
- Milota MR (1994) Specific gravity as a predictor of species correction factors for a capacitance-type moisture meter. *For Prod J* 44(3):63–68
- Nursultanov N, Altaner C, Heffernan WJB (2017) Effect of temperature on electrical conductivity of green sapwood of *Pinus radiata* (radiata pine). *Wood Sci Technol* 51(4):795–809
- Pérez-Marín D, Fearn T, Guerrero J, Garrido-Varo A (2012) Improving NIRS predictions of ingredient composition in compound feedingstuffs using Bayesian non-parametric calibrations. *Chemom Intell Lab Syst* 110(1):108–112

- Rantanen J, Räsänen E, Antikainen O, Mannermaa JP, Yliruusi J (2001) In-line moisture measurement during granulation with a four-wavelength near-infrared sensor: an evaluation of process-related variables and a development of non-linear calibration model. *Chemom Intell Lab Syst* 56(1):51–58
- Savitzky A, Golay MJE (1964) Smoothing and differentiation of data by simplified least squares procedures. *Anal Chem* 36(8):1627–1639
- Schimleck L, Mora C, Daniels R (2003) Estimation of the physical wood properties of green *Pinus taeda* radial samples by near infrared spectroscopy. *Can J For Res* 33(12):2297–2305
- Stienen T, Schmidt O, Huckfeldt T (2014) Wood decay by indoor basidiomycetes at different moisture and temperature. *Holzforschung* 68(1):9–15
- Tham VTH, Inagaki T, Tsuchikawa S (2018) A novel combined application of capacitive method and near-infrared spectroscopy for predicting the density and moisture content of solid wood. *Wood Sci Technol* 52(1):115–129. <https://doi.org/10.1007/s00226-017-0974-x>
- Thybring EE (2013) The decay resistance of modified wood influenced by moisture exclusion and swelling reduction. *Int Biodeterior Biodegrad* 82:87–95
- Thybring EE, Kymäläinen M, Rautkari L (2018) Experimental techniques for characterising water in wood covering the range from dry to fully water-saturated. *Wood Sci Technol* 52(2):297–329
- Tiitta M, Savolainen T, Olkkonen H, Kanko T (1999) Wood moisture gradient analysis by electrical impedance spectroscopy. *Holzforschung* 53(1):68–76
- Tsuchikawa S, Kobori H (2015) A review of recent application of near infrared spectroscopy to wood science and technology. *Wood Sci* 61(3):213–220
- Tsuchikawa S, Hayashi K, Tsutsumi S (1996) Nondestructive measurement of the subsurface structure of biological material having cellular structure by using near-infrared spectroscopy. *Appl Spectrosc* 50(9):1117–1124
- Watanabe K, Kobayashi I, Kuroda N, Harada M, Noshiro S (2012) Predicting oven-dry density of Sugi (*Cryptomeria japonica*) using near infrared (NIR) spectroscopy and its effect on performance of wood moisture meter. *Wood Sci* 58(5):383–390
- Wengert GAPB (1997) Evaluation of electric moisture meters on kiln-dried lumber. *For Prod J* 47(6):60–62
- Wilson PJ (1999) Accuracy of a capacitance-type and three resistance-type pin meters for measuring wood moisture content. *For Prod J* 49(9):29–32
- Windham W, Barton F, Robertson J (1988) Moisture analysis of forage by near infrared reflectance spectroscopy: preliminary collaborative study and comparison between Karl Fischer and oven drying reference methods. *J Assoc Off Anal Chem* 71:256–262
- Xu Q, Qin M, Ni Y, Defo M, Dalpke B, Sherson G (2011) Predictions of wood density and module of elasticity of balsam fir (*Abies balsamea*) and black spruce (*Picea mariana*) from near infrared spectral analyses. *Can J For Res* 41(2):352–358
- Yang Z, Liu Y, Pang X, Li K (2015) Preliminary investigation into the identification of wood species from different locations by near infrared spectroscopy. *BioResources* 10(4):8505–8517

**Publisher's Note** Springer Nature remains neutral with regard to jurisdictional claims in published maps and institutional affiliations.

## Affiliations

Vu Thi Hong Tham<sup>1,2</sup> · Tetsuya Inagaki<sup>1</sup> · Satoru Tsuchikawa<sup>1</sup>

✉ Satoru Tsuchikawa  
st3842@agr.nagoya-u.ac.jp

<sup>1</sup> Graduate School of Bioagricultural Sciences, Nagoya University, Furo-cho, Chikusa-ku, Aichi 464-8601, Japan

<sup>2</sup> Forest Industry Research Institute, Vietnam Forest Academy, Dong Ngạc, Tu Liem, Vietnam